231646

UCRL-JC-126283
PREPRINT

Radiant Transmittance of Cerium Doped Quartz from 300 to 1270K

Mark A. Havstad
Charles Dingus

This paper was prepared for submittal to the
National Heat Transfer Conference of the American Society of Mechanical Engineers
Baltimore, Maryland
8/10-12/97

Manuscript Date 3/14/97

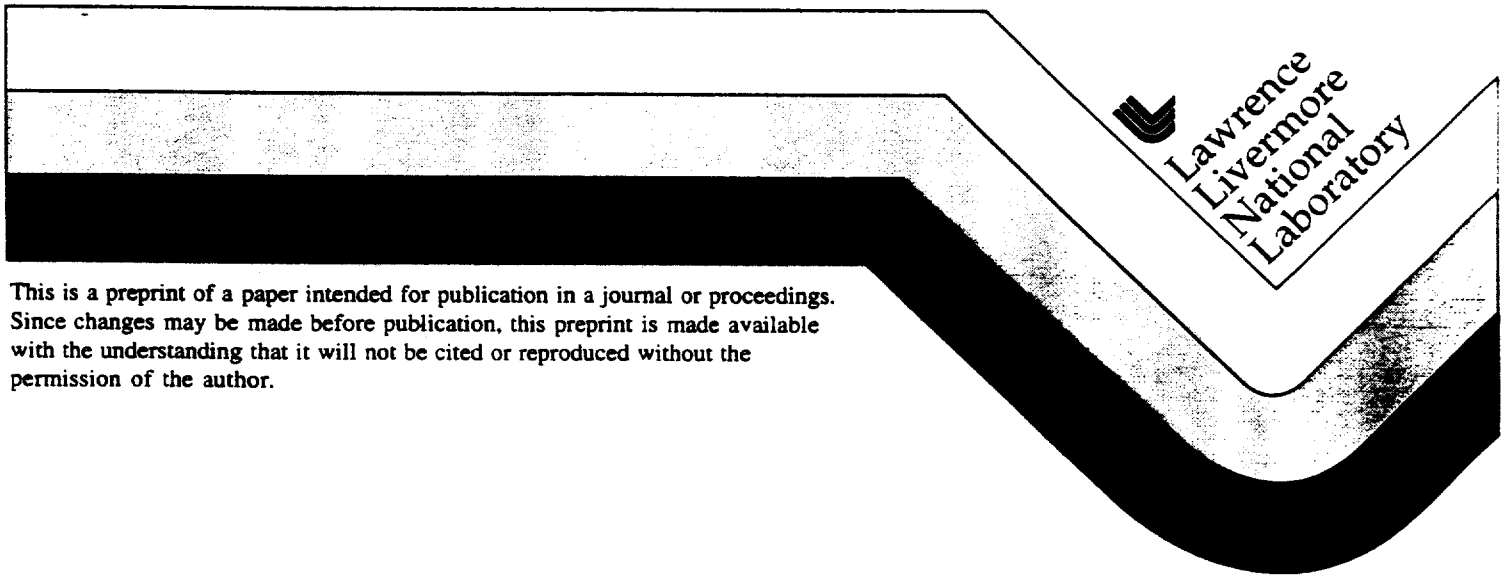

DISCLAIMER

Radiant Transmittance of Cerium Doped Quartz from 300 to 1270 K

Mark A. Havstad
Laser Sciences Engineering Division, Lawrence Livermore National Laboratory,
Livermore, California,USA

Charles Dingus
8160B North Lake Drive,
Dublin, California,USA

ABSTRACT

The transmittance of curved slabs of cerium doped quartz is reported as a function of wavelength and temperature. The spectral range of measurement is 0.25 to 0.725 μm and temperature varies from 300K to 1270K. The short wavelength cutoff for transmission shifts to longer wavelengths monotonically with temperature at a rate of ~3nm/100K. The transmittance data for wavelengths less than 0.36 μm are fit to a classical pole fit model using 8 modes (oscillators) and the temperature dependence of the modes is given. For wavelengths beyond 0.36 μm the data are fit to an "Urbach rule." The bandgap parameter in the Urbach rule decreases linearly with temperature to 1270K and varies from 3.394eV at 300K to 3.183 eV at 1270K, while the steepness parameter also decreases approximately linearly from 8.51 eV^{-1} to 5.80 eV^{-1}. The fits are used to compute the spectral and temperature dependent absorption coefficient.

INTRODUCTION

Small amounts of transition or rare earth elements in fused quartz can result in preferred radiation transmission properties for several applications. Klimashina and Chistoserdov (1975) reported the room temperature transmission in the ultraviolet and visible of quartz doped with Ce, Ti, Sn and Eu. Dopant concentration varied to as high as 0.6% as part of a search for improved laser and specialty optical glasses. Laczka and Stoch (1988) reported absorption in the UV and visible of quartz doped with Ce, Ti and Nd (to 0.2%) with similar motivation. These studies and others led to the use of cerium doped quartz in the envelopes of flashlamps used as optical pumps in laser systems.

A particularly massive application of cerium doped quartz flashlamps is scheduled as part of the fusion energy research program at the National Ignition Facility (NIF) to be built at the Lawrence Livermore National Laboratory (LLNL). As many as 10,000 flashlamps will fire in support of each laser driven fusion experiment. Over the 350 μsec firing period, the lamps provide visible and IR output (the pump band is 0.4 to 1.0μm) to a solid state laser slab. Emission from the lamp toward its envelope corresponds roughly to a 10,000 K Planck distribution and causes envelope heating to approximately 1070 K.

Temperature dependent radiation transmission by the doped glass envelope is important to lamp performance and laser operation for several reasons. UV transmission through the envelope can cause damage and limit the useful life of the laser slab and other components. Pump band transmission influences system efficiency and cost. Transmission at wavelengths beyond the pump band causes laser slab heating which gives laser beam distortion, reduces the frequency with which fusion experiments can occur and can cause laser slab fracture.

Temperature dependent absorption in the lamp envelopes may influence lamp failure during firing. Occasionally failures occur early in a lamp's expected lifetime and the positive feedback loop constituted by lamp absorption (lamp heating causes enhanced absorption which causes more heating) may play a part in these failures.

Since no quantitative data on the temperature dependence of absorption or transmission of cerium doped quartz are available, our objective here is to obtain the temperature and spectral dependence of the transmission of cerium doped quartz from 250 to 725 nm and from ambient to 1270 K. Of particular concern are the 1) change in transmission in the pump band during the rise in temperature during firing, 2) the change in transmission in the UV due to heating and 3) expressing the doped glass properties in a form which facillitates use in computer modelling so that the temperature, spectral and spatial dependence of transmission and absorption in the envelopes can be computed and used with transient thermal stress analysis.

In order to independently determine two distinct optical properties of a material (e.g. the index of refraction and the absorption coefficient) it is necessary, of course, to make two independent measurements. Hence one measures the transmission of two different thickness slabs of the same material or one makes both a reflection and a transmission measurement on a single slab and from them one deduces the real and imaginary components characterizing wave propagation in a material. Methods for determining the two optical constants from a single measurement are however also heavily used and with good reason. The Kramers-Kronig relations permit the computation of both the real and imaginary parts of a material's optical constants from a single measurement provided that the single measurement is performed over a sufficiently broad spectral region (in theory infinity) (Bohren and Huffman, 1983). A single measurement can also be used

provided one makes a more direct assumption about the relationship between the real and imaginary components (in this case one is not independently determining the two optical properties). Thomas (1991) gives several forms in use for the relationship between the two optical constants and notes that all possible forms are not equal; those forms which satisfy the Kramers-Kronig relations are preferred.

In this work a number of practical considerations (to be discussed below) have led us to make a single transmittance measurement. In the UV and short wavelength portion of the visible (to ~.360 μm) we have assumed a classical "pole fit model" for the relationship between the optical constants. The pole fit model is equivalent to the classical harmonic oscillator model of Lorentz for optical absorption, long supplanted by quantum formulations but we use it here to satisy the objectives outlined above. For wavelengths beyond ~.360 μm we have used the Urbach model for the absorption edge (Lynch, 1985).

Principal among practical considerations which led to our use of a single measurement for the determination of the optical constants was the available material. The cerium doped quartz of interest was only available in a single thickness (2.5 mm) and that in tubing form of O.D. 75 mm. This constraint is probably not as unique as one might expect at first look. Material which has failed in some application, particularly with an exploded flashlamp, is clearly of more interest and may be more information bearing than normal material: the failed material may be the only material containing the explanation of the failure. A measurement method capable of examining failed material from actual use was chosen here. Furthermore, it is well known that the fabrication process for many optical materials can strongly influence the optical properties. The flashlamp tubes of interest here are drawn to the final thickness and diameter from larger diameter tubes in a unique commercial process. A method using flat slabs, or any other form of the material might have been theoretically superior but could have resulted in work with material qualitatively different than that in actual use.

APPARATUS

The optical system (shown in Fig. 1) was designed to be used over a broad spectral range, 0.2 to 9.0 μm. The carbon filament lamp (Havstad et. al., 1993) (power usage 24 amps at 12 volts d.c.), imaged along the vacuum furnace axis by the spherical mirror on a kinematic base, is useful in the visible and IR. The arc lamp (200w mercury-xenon bulb), imaged by a UV grade fused silica lens, provides UV, visible and near IR output. For visible and UV measurements the carbon lamp is off and the spherical mirror is removed from the kinematic base. This arrangement allows both light sources to be imaged down the furnace axis and once aligned to be fixed in position. Apertures along this optic axis limit the beam to a diameter of 0.6 mm.

The furnace includes a 102mm long by 64mm diameter heating element (0.64 mm thick carbon composite) which dissipates 600 watts of d.c. power at 21 amps to give sample temperatures of 1270 K. Samples are held in graphite rings which are supported by four alumina rods which span the axial length of the hot zone and are themselves supported by the niobium thermal shields at either end of the furnace. A clear aperture of 12.7 mm diameter is bored through the thermal shields for the transmitted beam but larger beams could be accommodated; the graphite rings holding the sample allow a clear aperture through the sample as large as 40 mm. Five layers of thermal shielding are used at the furnace ends and around the furnace circumference. These last shields isolate the hot zone from a water cooled jacket which is fitted between the shields and the vacuum vessel wall.

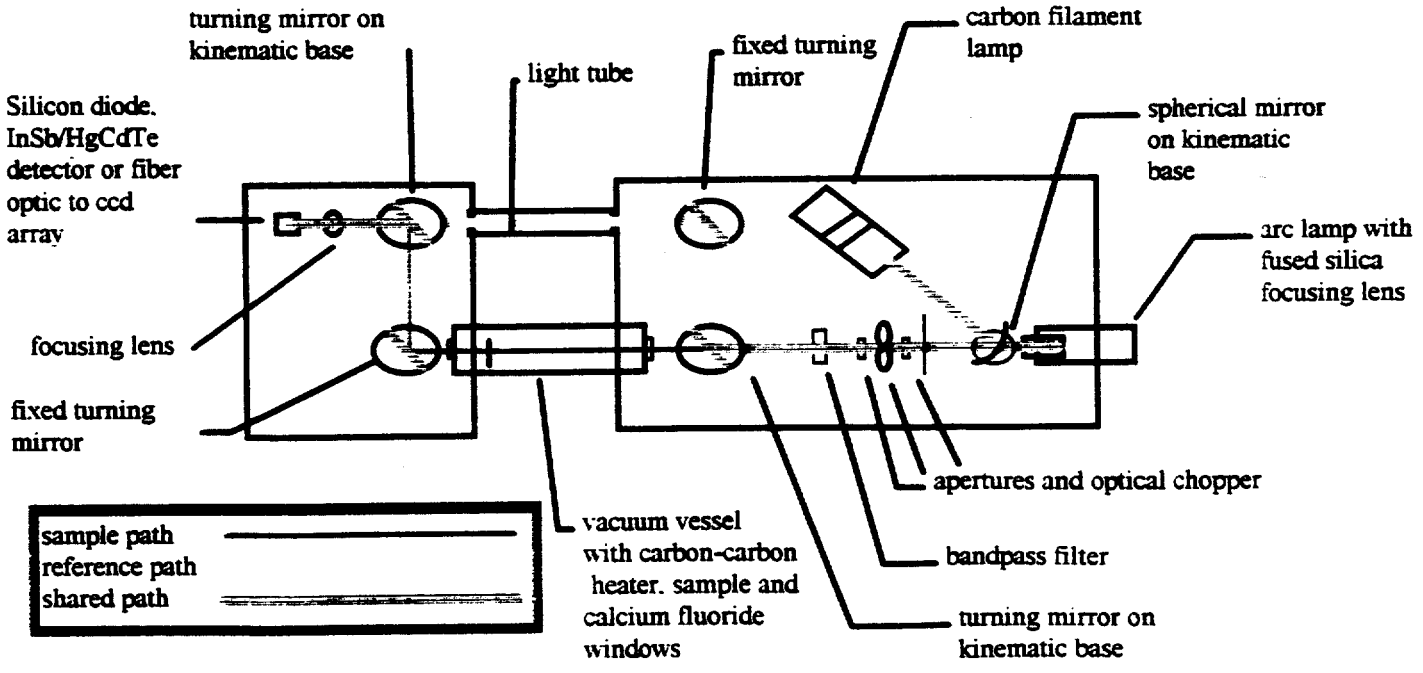

Figure 1 Schematic of the apparatus

The furnace is pumped by a 60 l/s turbomolecular pump backed by a mechanical roughing pump. The windows for optic access are calcium fluoride disks mounted in conflat vacuum flanges by a proprietary silver brazing process. The window on the entrance side is mounted in a 33.8 mm O.D. flange and has a clear aperture of 11.8 mm and on the exit side a 69.8 mm flange with a clear aperture of 32.4 mm

The optical system uses two beam paths; a sample path where the beam passes through the furnace and the sample, and a reference path where the beam is diverted by a turning mirror and routed to the detector by a path which remains at essentially room temperature for the duration of the measurements. The reference path (~210 cm long) is equal in length (to within about 1 cm) to the sample path and the two turning mirrors in each path were fabricated on the same coating run. The focusing lens, filter and detectors common to the two beam paths are relatively isolated from the furnace thermal emission.

During initial optical alignment through the furnace the output of the two light sources is imaged on the far wall of the laboratory so that the light incident on the sample is nearly collimated. Since the turning mirrors are all planar, the thermal emission from the furnace is not imaged at the detector and its intensity declines as the square of the distance from the furnace to the focusing lens.

The CaF_2 focusing lens images either of the light sources on the detection optics. For spectrally coarse measurements a bandpass filter is placed between the the lens and a silicon photodiode or an InSb/HgCdTe sandwich detector. For this system the chopper, a lock-in amplifier and a diode preamp make up a phase sensitive detection system. For more spectrally resolved measurements (0.25 to 0.725 μm) the transmitted beam is imaged into an optical fiber. The fiber extends to a commercially supplied computer board. At the board back plane are a lens, a miniature grating and a 1024 element ccd detector array. The spectral calibration (pixel number to wavelength) is provided with the board and can be checked with any light source with known, sharp spectral lines.

The detector response for the sample and beam paths (minus the system dark signal) can be represented by:

$$V_{sam} - V_{dar} = B\tau_{w1}\tau_{sam}\tau_{w2}\rho_{T1}\rho_{T2}\tau_L\tau_f R \qquad (1)$$

$$V_{ref} - V_{dar} = B'\rho_{T3}\rho_{T4}\tau'_L\tau'_f R' \qquad (2)$$

Where ρ is the turning mirror reflectance, τ is transmittance, R is detector responsivity and B is lamp output through the chopper and apertures. Subscripts L,f, T1, T2, T3 and T4 refer to the focusing lens, bandpass filter and turning mirrors. Subscripts W1 and W2 refer to the entrance and exit windows on the furnace. The use of a prime on some of the symbols indicates a second order deviation between the primed and unprimed values. For example, the transmittance of the focusing lens is nominally the same for either beam path but small differences in beam size or incident angle for example, result in slight deviations.

At any given wavelength and sample temperature the ratio of transmittance at temperature to the transmittance at room temperature is computed from the above two relations:

$$\frac{\tau(Temp)}{\tau(amb)} = \frac{\left(\frac{B\tau_{w1}\tau_{sam}\tau_{w2}\rho_{T1}\rho_{T2}\tau_L\tau_f R}{B'\rho_{T3}\rho_{T4}\tau'_L\tau'_f R'}\right)_{temp}}{\left(\frac{B\tau_{w1}\tau_{sam}\tau_{w2}\rho_{T1}\rho_{T2}\tau_L\tau_f R}{B'\rho_{T3}\rho_{T4}\tau'_L\tau'_f R'}\right)_{amb}} \qquad (3)$$

Thus the apparatus is used to make a relative transmittance measurement, τ_{temp}/τ_{amb}. A Cary 5 spectrophotometer was used to make a precision absolute transmittance measurement at room temperature. Errors and uncertainties arising in this apparatus are largely due to drift in the light source output and thermal emission from the vacuum vessel (both these effects dominate the small nonlinearity of the detector response for any of the three types of detector cited in Fig. 1).

RESULTS

The temperature dependent transmittance of a cerium doped quartz sample provided from NIF development operations is shown in Fig. 2. Absorption in the UV and short wavelength portion of the visible increases with temperature. This increase in absorption is desirable from the viewpoint of reducing damaging UV passed from a flashlamp to the remainder of its laser system and is probably inconsequential to lamp failure mechanisms - it would take a much larger effect with temperature to account for lamp heating leading to explosion. The change in the integral of the product of the transmittance and the Planck function over the wavelengths measured is only 4 % (the fraction of blackbody radiation in the pumpband (for a 10000 K Planck distribution) is ~0.43 while the fraction in the measurement range here (0.248 to 0.725 μm) is ~.66). The shift in the absorption edge to longer wavelengths is unwanted because it reduces pump band output but the shift noted here is modest and most of it confined to wavelengths less than those designated pump band in the NIF application.

A second unwanted but also modest effect is the absorption at .500 μm. This feature as well as the weak temperature dependent absorption at .400 μm was observed in work with coarse spectral resolution (bandpass filters) but here it is better quantified. The longer wavelength data indicate that there are no absorption phenomena beyond .550 μm of significance (as was indicated by work with bandpass filters also) but quantitatively the indication of higher transmittance at elevated temperature than at ambient is probably incorrect (due to declining signal to noise ratio as furnace emission increases with temperature). The short wavelength cutoff in transmission shifts to longer wavelengths steadily at a rate of approximately 3 nanometers per 100 K and the slope of the cutoff becomes less steep monotonically with temperature.

In contrast to the curves of Fig. 2. the transmittance of undoped quartz remains near 0.9 over most of a band stretching from 0.2 to 2.0 μm. Data obtained using bandpass filters (miscellaneous wavelengths scattered from 0.7 to 8.0 μm) and the carbon filament lamp indicated no significant changes in transmittance with temperature due to the cerium dopant (other than what is shown in Fig. 2).

The precision of the results shown for transmittance varies strongly with wavelength. In the .25 to .33 μm range the results are uncertain to within ~±.03. This uncertainty, largely due to the weak

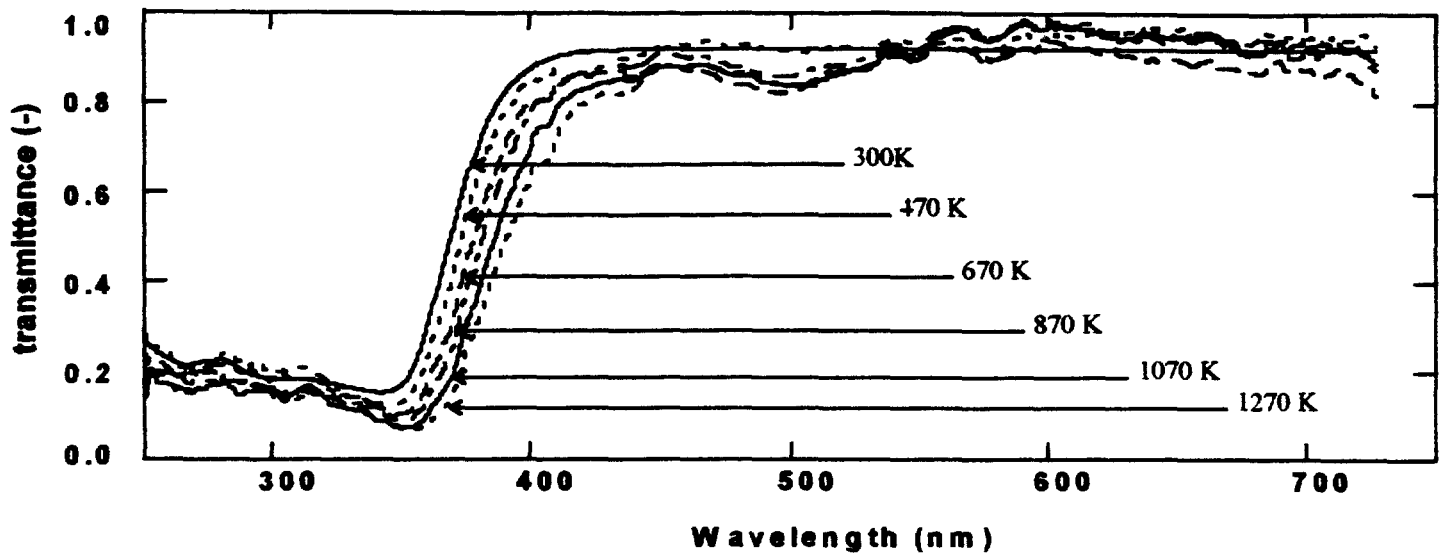

Figure 2 Transmittance of cerium doped quartz from 300 to 1270 K

output of the arc lamp source in the UV, is consistent with the rule of thumb that the root mean square deviation is approximately one quarter of the peak to peak variation in the signal (Lichten, 1988). In the 0.33 to .55 μm range a similar approach gives an uncertainty of ~±.01, but the results shown below for the fit to the data in the absorption edge imply a significantly lower uncertainty. In the 0.55 to 0.725 μm range the peak to peak variation implies an uncertainty on the order of ±.05, in part because thermal output from the furnace is reaching the detector.

Optical constants, which determine a material's transmittance, are typically formulated in one of several ways; e.g. the index of refraction, n, and the extinction coefficient, k, or the index and the absorption coefficient, $\mu = 4\pi k/\lambda$ (k is sometimes also referred to as the absorption index). The extinction coefficient is dimensionless while the absorption coefficient is most often given in inverse centimeters. A pole-fit model (or a collection of Lorentz oscillators) for the optical constants has the form:

$$\varepsilon^c = \varepsilon_{\infty} - \sum_{j=1}^{p} \frac{\nu_j^2 \Delta\varepsilon_j}{\nu_j^2 - \nu^2 + i\nu\gamma_j} \qquad (4)$$

The complex permittivity is ε^c (yet another pair constituting the optical constants), ν is the wavenumber (the inverse of the wavelength) in cm^{-1}, $\Delta\varepsilon_j$ is the mode strength, ν_j is the mode (oscillator resonant frequency) and γ_j is the line width (damping constant). The static dielectric constant is ε_{∞} and p is the number of modes. All quantities except the wavenumber and p are functions of temperature. This relation satisfies the Kramers-Kronig relations and thus provides a physically consistent relationship between the two optical constants (Thomas, 1991). The choice of a few of the modes is somewhat arbitrary (each mode is not identifiable with a particular minimum in the transmittance) but the parameters given in table 1 give a reasonable fit to the transmittance data. Values of mode strength and line width were computed in a routine embedded in a MATHCAD program. Modes were assigned for the locations where the transmittance displayed a local minimum and then several more were added to improve the match to the transmittance curves. The program returns values of mode strength and line width for two of the defined modes upon each execution (the square of the difference between measured and calculated transmittance is minimized). Execution is repeated for different pairs of defined modes until strength and line width have converged for all 8 defined modes.

The index of refraction computed from the pole fit model is physically reasonable (a standard reference on optics (Jenkins and White, 1976) gives the index of undoped fused quartz as varying from 1.504 at .257 μm to 1.455 at .707 μm), however more conventional measurement methods give far more precise and accurate values for n (Driscoll and Vaughan, 1978). For the present objectives, the dependence of n on wavelength and temperature shown is sufficiently weak that the reflectance of this material will be taken as constant in the fit of the longer wavelength data (extinction coefficient is sufficiently small that n determines reflectance).

For wavelengths beyond .360 μm the absorption edge is well fit by the "Urbach rule" (Lynch, 1985):

$$\mu(\nu, T) = \mu_{amb} \exp\{-b(T)[E_g(T) - E(\nu)]\} \qquad (5)$$

$$\tau(\nu, T) = (1-\rho)^2 \exp\{-\mu(\nu, T)t\} \qquad (6)$$

The absorption coefficient at ambient is μ_{amb}, photon energy is E=hν, E_g is the bandgap and b is the steepness parameter. The slab thickness is t and ρ is the reflectance (here assumed independent of n and T because of the weak dependence of n on ν and T discussed

Table 1 Harmonic oscillator parameters as a function of temperature

mode number	Oscillator mode, ν, in nanometers as a function of temperature					
(-)	300K	470K	670K	870K	1070K	1270K
1	338	338	338	338	338	338
2	347	349	350	351	353	355
3	280	280	280	280	280	280
4	313	313	313	313	313	313
5	335	335	335	335	335	335
6	263	263	263	263	263	263
7	252	252	252	252	252	252
8	300	300	300	300	300	300
	Line width (damping) divided by oscillator frequency (dimensionless)					
1	0.027	0.071	0.05	0.039	0.031	0.055
2	0.043	0.054	0.064	0.058	0.063	0.065
3	0.2	0.2	0.2	0.2	0.2	0.2
4	0.15	0.15	0.15	0.15	0.15	0.15
5	0.3	0.3	0.3	0.3	0.3	0.3
6	0.12	0.12	0.12	0.12	0.12	0.12
7	0.04	0.04	0.04	0.04	0.04	0.04
8	0.319	0.319	0.319	0.319	0.319	0.319
	Mode strength (dimensionless)					
1	0.138	0.467	0.2	0.116	0.182	0.394
2	0.618	0 796	1.616	2.107	2.514	3.404
3	0.7	0.8	0.8	0.7	0.8	0.7
4	0.3	0.4	0.4	0.3	0.4	0.3
5	8	8.7	8.7	8	9	7
6	1.5	1.9	1.9	1.8	2	1.9
7	0.3	0.4	0.4	0.3	0.5	0.3
8	7.02	7.25	7.25	7.02	7.5	6

above). Equation (6) is an approximation to the slab transmission including internal reflections (Bohren and Huffman, 1983) which holds here given the sample thickness, index of refraction and low extinction coefficient. Various explanations for the Urbach rule's dependence of the absorption edge on wavelength have been given, including thermal fluctuation of the bandgap (Skettrup, 1978) and electric fields arising from defects, phonons and impurities (Dow and Redfield, 1972).

The transmittance data for ambient has been fit (for wavelengths from 0.36 to 0.45 μm) to the two equations above with four parameters varied (ρ, E_g, b and μ_{amb}) until the sum of the squared error was minimized. The data at elevated temperatures was fit similarly but with ρ fixed (at 0.039, the result obtained for ambient temperature) and the last three variables minimized. The results of these fits are given in Table 2. With the exception of the data for 1270 K, μ_{amb} is approximately constant and the other two vary approximately linearly with temperature. The shift of E_g with temperature, a shift of the Urbach tail to longer wavelengths, is shown in Fig. 3. The addition of cerium has reduced the bandgap considerably (undoped quartz, has a bandgap of ~7.8 eV) and made it temperature dependent. For many materials, the bandgap in the Urbach rule is the bandgap at zero Kelvin and it is temperature independent.

Table 2 Urbach tail parameters as a function of temperature

Temperature (K)	μ_{amb} (1/cm)	b (1/eV)	E_g (eV)
300	308	8.51	3.394
470	309	8.13	3.358
670	319	6.77	3.322
870	312	7.09	3.293
1070	302	6.32	3.248
1270	261	5.80	3.183

The dependence of the steepness parameter on temperature, shown in Fig. 4, is less strongly correlated to a linear fit (the coefficient of determination is 0.907 for b compared to 0.983 for E_g) but still well fit. In some materials b is a constant while in the alkali halides and others a more complex dependence on temperature (a product of a term linear in temperature and a term with an inverse dependence on temperature inside a hyperbolic tangent) (Lynch, 1985) is used.

The transmittance data is compared to calculations based on the relations given above, for two sample temperatures, 300 K and 1270 K in Fig. 5. Comparison between the fits and the data at other temperatures is similar to that shown for 1270 K. Better data in the .500 to .725 μm range is required to justify more detailed modelling of the absorption in this band.

The oscillator and Urbach models allow a compact specification of both the transmittance and the absorption coefficient (the latter is useful to computer modelling of radiant transport and transient thermal stress in a flashlamp envelope). The absorption coefficient computed from the parameters in Tables 1 and 2 is plotted in Fig. 6 for four temperatures. The close match between the pole fit and Urbach models around .360 μm is a necessary though not sufficient condition for validating the various assumptions in the calculation of absorption coefficient from the transmittance data. The

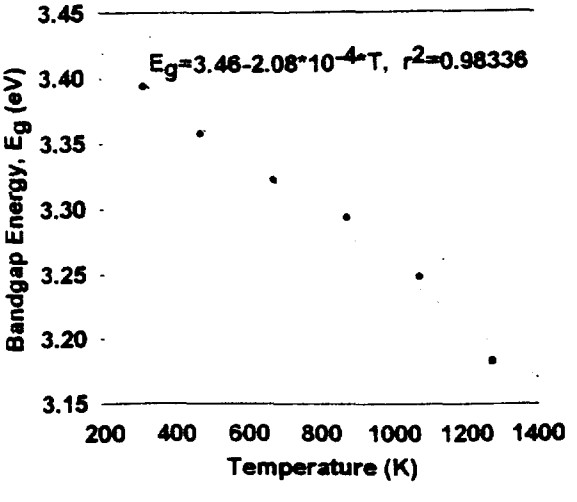

Figure 3 Bandgap energy of Urbach fit as a function of temperature for cerium doped quartz

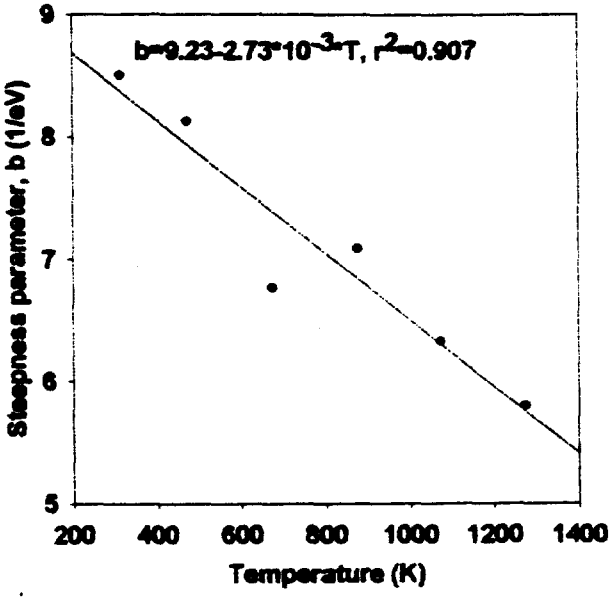

Figure 4 Steepness parameter of Urbach fit as a function of temperature for cerium doped quartz

only results shared between the pole fit and Urbach models for any given temperature were that 1) the extinction coefficient was so low as to make a negligible contribution to reflectance and 2) the index of refraction varied so weakly with temperature and wavelength that reflectance above .360 μm was constant. For wavelengths less than .250 μm other data or models are required; the increase in the absorption coefficient below .250 μm contributes significantly to the heat load in the flashlamp application.

Participating media calculations of transport through the thickness of a flashlamp envelope using the Monte Carlo approach (Maltby, 1994) and transient thermal stress calculations by the finite element method using temperature independent properties have been performed (Maltby et. al., 1996).

SUMMARY

The first reported measurements of the transmittance of cerium doped quartz at elevated temperature show a moderate decrease with temperature in the UV, a shift in the absorption edge to longer wavelengths and a weak absorption feature at ~0.5 μm.

The absorption edge is well fit by an Urbach rule with temperature dependent bandgap and steepness parameters. Because the arc within typical flashlamps is characterized by a ~10,000 K Planck distribution, data for transmittance below 0.25 μm would be interesting. However, it would require significantly different equipment.

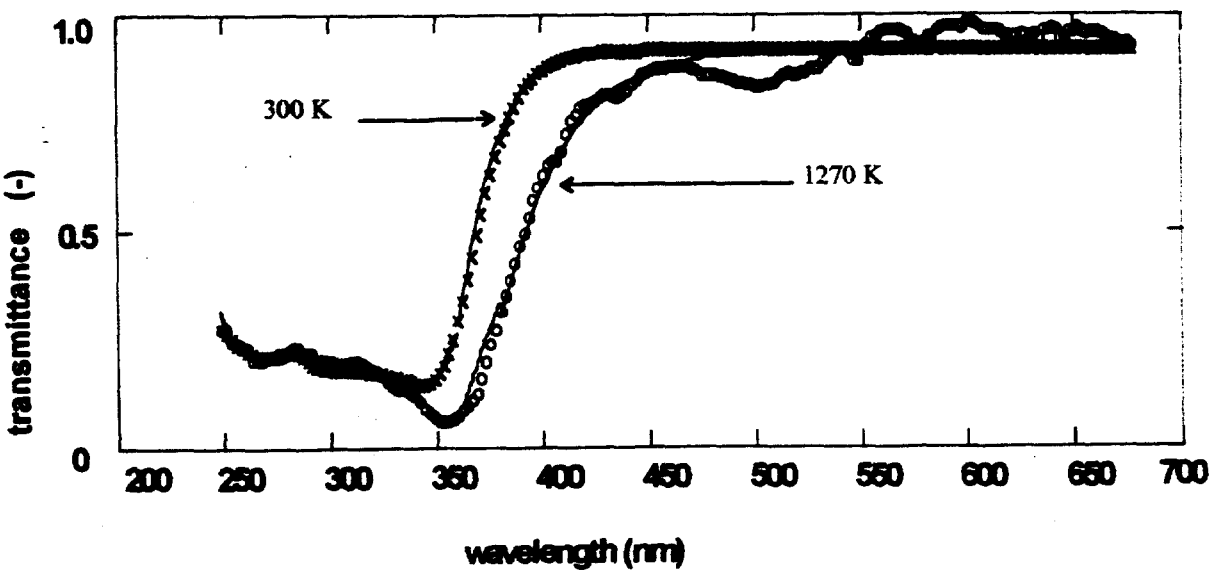

Figure 5 Comparison of measurements and fits for the transmittance of cerium doped quartz

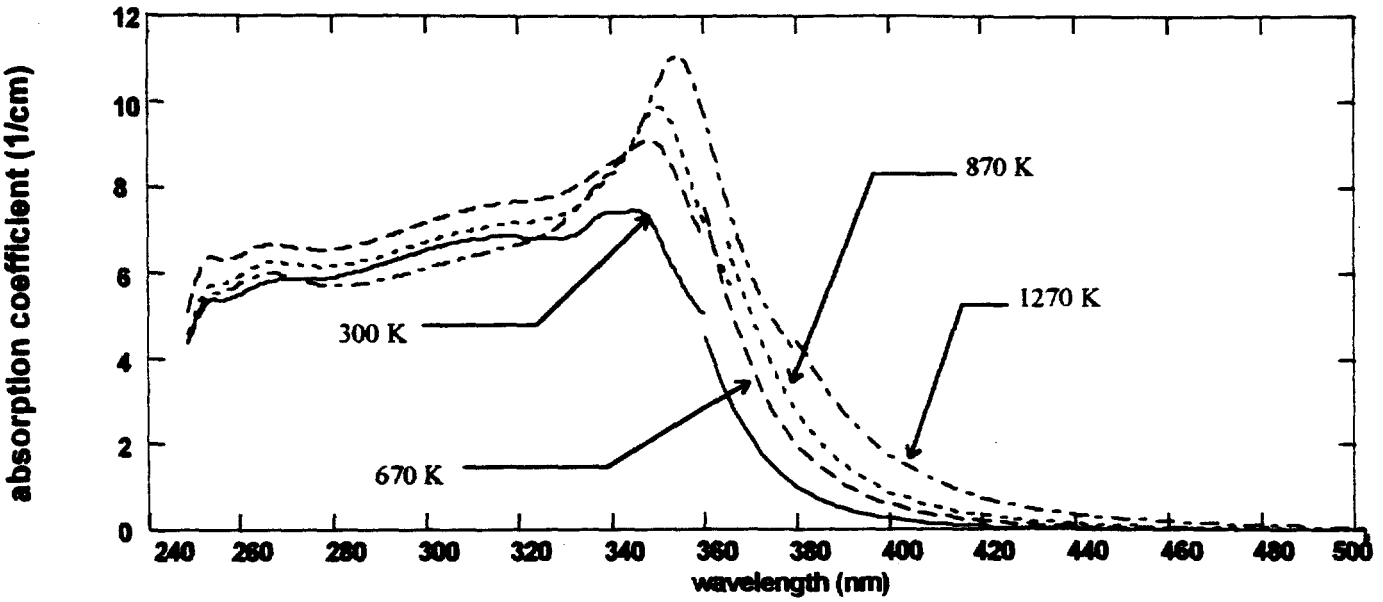

Figure 6 Absorption coefficient of cerium doped quartz as a function of wavelength with temperature as a parameter

REFERENCES

Bohren, C. F. and Huffman , D. R., 1983, Absorption and Scattering of Light by Small Particles, John Wiley and Sons, New York.

Dow, J. P., and Redfield, D., 1972, "Toward a unified theory of Urbach's Rule and exponential absorption edges," Phys. Rev. B, Vol. 5, pp. 594-610.

Driscoll, W. G., and Vaughan, W., 1978, Handbook of Optics, McGraw-Hill, New York.

Havstad, M. A., Self, S. A., Brown, D. L., Maltby, J. D., and Ebert, J. L., 1993, "A Radiant Source for Both the Visible and the Infrared," Infrared Physics, Vol. 34, pp. 169-174.

Jenkins, F. A., and White, H. E., 1976, Fundamentals of Optics, McGraw-Hill, New York.

Klimashina, E. V., and Chistoserdov, V. G., 1975, "Effect of small Additions of some Elements on the Spectral Properties of Vitreous Silica," Soviet Journal of Glass Physics and Chemistry, Vol. 1, pp. 144-146.

Lacza, M., and Stoch, L., 1988, "Synthesis, Structure and Electron Spectra of Fused Quartz Doped with Titanium, Cerium and Neodymium," Glastech Ber., Vol. 61, pp. 218-222.

Lichten, W., 1988, Data and Error Analysis, Allyn and Bacon, Boston.

Lynch, D. W., 1985, "Interband Absorption - Mechanisms and Interpretation," in Handbook of Optical Constants of Solids, Academic Press, New York, pp. 189-212.

Maltby, J. D., 1994, "Evaluation of Property-induced Uncertainty in a Monte Carlo Simulation of Radiative Heat Transfer in a Participating Medium," Radiative Heat Transfer: Current Research, ASME HTD-Vol 276, New York.

Maltby, J. D., Garcia, V. C. and Kornblum, B. T., 1996, "Radiation-Induced Thermal Stresses in High-Power Flashlamps," Engineering Research, Development and Technology, Lawrence Livermore National Laboratory, Livermore, Calif., UCRL-53868-96.

Skettrup, T., 1978, "Urbach's Rule derived from Thermal Fluctuations in the Band Gap Energy," Phys. Rev. B, Vol. 18, pp. 2622-2631.

Thomas, M. E., 1991, "Temperature Dependence of the Complex index of Refraction," in Handbook of Optical Constants of Solids II, Academic Press, New York, pp. 177-201.

*This work was performed under the auspices of the U.S. Department of Energy by Lawrence Livermore National Laboratory under contract No. W-7405-Eng-48.

NOMENCLATURE

b	steepness parameter in Urbach fit (1/eV)
B	output from light source through initial apertures (watts)
E	photon energy (eV)
E_g	bandgap (eV)
i	imaginary number
j	oscillator index
k	extinction coefficient
n	real component of index of refraction
p	number of oscillators in fitting model
R	responsivity of detector (volts/watt)
t	thickness of material (cm)
T	temperature (K)
V	detector output (volts)
τ	transmittance
ε^c	complex dielectric constant
λ	wavelength (nm or μm)
ν	frequency of radiation (1/cm)
ν_j	oscillator mode (frequency of resonance) (1/cm or nm)
ρ	reflectance
$\Delta\varepsilon_j$	mode strength
γ_j	line width (damping constant) (cm^{-1})
μ	absorption coefficient (1/cm)

SUBSCRIPTS

amb	ambient
c	complex
dar	dark
f	filter
j	index for oscillator
L	lens
ref	reference

Technical Information Department • **Lawrence Livermore National Laboratory**
University of California • Livermore, California 94551